The Plant Cell, Vol. 16, 45–59, January 2004, www.plantcell.org © 2003 American Society of Plant Biologists

γ-Tubulin in Basal Land Plants: Characterization, Localization, and Implication in the Evolution of Acentriolar Microtubule Organizing Centers

Masaki Shimamura,[a,b] Roy C. Brown,[c] Betty E. Lemmon,[c] Tomohiro Akashi,[d] Koichi Mizuno,[e] Naohisa Nishihara,[a] Ken-Ichi Tomizawa,[b] Katsuhiko Yoshimoto,[f] Hironori Deguchi,[a] Hiroshi Hosoya,[a] Tetsuya Horio,[g] and Yoshinobu Mineyuki[a,1]

[a] Department of Biological Science, Graduate School of Science, Hiroshima University, Higashi-Hiroshima 739-8526, Japan
[b] Plant Molecular Physiology Laboratory, Research Institute of Innovative Technology for the Earth, Kizu, Kyoto 619-0292, Japan
[c] Department of Biology, University of Louisiana, Lafayette, Louisiana 70504
[d] Division of Molecular Mycology and Medicine, Nagoya University Graduate School of Medicine, 65 Tsurumai, Nagoya 466-8550, Japan
[e] Department of Biology, Graduate School of Science, Osaka University, Toyonaka, Osaka 560-0043, Japan
[f] Otsuka Department of Molecular Nutrition, School of Medicine, University of Tokushima, Tokushima 770-8503, Japan
[g] Department of Nutrition, School of Medicine, University of Tokushima, Tokushima 770-8503, Japan

Although seed plants have γ-tubulin, a ubiquitous component of centrosomes associated with microtubule nucleation in algal and animal cells, they do not have discrete microtubule organizing centers (MTOCs) comparable to animal centrosomes, and the organization of microtubule arrays in plants has remained enigmatic. Spindle development in basal land plants has revealed a surprising variety of MTOCs that may represent milestones in the evolution of the typical diffuse acentrosomal plant spindle. We have isolated and characterized the γ-tubulin gene from a liverwort, one of the extant basal land plants. Sequence similarity to the γ-tubulin gene of higher plants suggests that the γ-tubulin gene is highly conserved in land plants. The G9 antibody to fission yeast γ-tubulin recognized a single band of 55 kD in immunoblots from bryophytes. Immunohistochemistry with the G9 antibody clearly documented the association of γ-tubulin with various MTOC sites in basal land plants (e.g., discrete centrosomes with and without centrioles and the plastid surface in monoplastidic meiosis of bryophytes). Changes in the distribution of γ-tubulin occur in a cell cycle–specific manner during monoplastidic meiosis in the liverwort *Dumortiera hirsuta*. γ-Tubulin changes its localization from the plastid surface in prophase I to the spindle, from the spindle to phragmoplasts and the nuclear envelope in telophase I, and back to the plastid surfaces in prophase II. In vitro experiments show that γ-tubulin is detectable on the surface of isolated plastids and nuclei of *D. hirsuta*, and microtubules can be repolymerized from the isolated plastids. γ-Tubulin localization patterns on plastid and nuclear surfaces are not affected by the destruction of microtubules by oryzalin. We conclude that γ-tubulin is a highly conserved protein associated with microtubule nucleation in basal land plants and that it has a cell cycle–dependent distribution essential for the orderly succession of microtubule arrays.

INTRODUCTION

γ-Tubulin is the third member of the tubulin superfamily, with ~30% amino acid sequence identity with α- and β-tubulins (Oakley and Oakley, 1989). Although α- and β-tubulin heterodimers are major components of microtubules, γ-tubulin is restricted to the minus ends of microtubules at the microtubule organizing centers (MTOCs) in eukaryotic cells, where it is thought to play an essential role in microtubule nucleation (reviewed by Oakley, 2000). A typical MTOC in animal and algal cells is the centrosome, a compound structure composed of a central centriole pair embedded in an amorphous matrix with astral microtubules radiating from it. The pericentriolar material is important in the nucleation of microtubules and in spindle pole formation in mitosis. Microtubules always have their stable minus ends toward the centrosome and their plus ends facing outward (Heidemann and McIntosh, 1980). γ-Tubulin is enriched in MTOC sites, where it appears to associate specifically with several other proteins to form larger ring-shaped complexes. These γ-tubulin rings enhance the nucleation of microtubules and set up minus-end proximal polarity of microtubules relative to animal centrosomes and fungal spindle pole bodies (Horio et al., 1991; Stearns et al., 1991; Zheng et al., 1991, 1995). Numerous experimental studies have provided evidence for an important role of γ-tubulin in centrosome function (Felix et al., 1994; Stearns and Kirschner, 1994; Shu and Joshi, 1995). For example, microinjection of γ-tubulin antibody disrupts both the nucleation of new microtubules from the centrosome and the morphogenesis of the mitotic spindle (Joshi et al., 1992; Joshi and Zhou, 2001).

[1] To whom correspondence should be addressed. E-mail mineyuk@hiroshima-u.ac.jp; fax 81-824-24-0734.
Article, publication date, and citation information can be found at www.plantcell.org/cgi/doi/10.1105/tpc.016501.

Typical land plant cells, however, have no MTOCs comparable to centrosomes. Instead, nucleation sites for microtubules appear to be distributed on the cytoplasm and/or a variety of endomembranes, including endoplasmic reticulum and nuclear and plastid envelopes, and relocate in a cell cycle–specific manner. Dividing vegetative cells of vascular land plants are characterized by an orderly succession of microtubule arrays. Five distinct microtubule systems generally are recognized: radial arrays from the nuclear surface, cortical arrays of interphase, preprophase bands, spindles, and phragmoplasts. As is evident from the recent direct observation of cortical microtubule dynamics by Shaw et al. (2003), MTOCs of seed plants are diffuse and migratory. This fact made it difficult to identify homology with models based on animal cells, in which the MTOC is closely associated with easily identified centrosome (Palevitz, 1993).

The oldest living lineage of land plants, the bryophytes (mosses, liverworts, and hornworts), represent a pivotal group for considering the evolution of land plants. Although the five microtubule systems mentioned above are found in bryophytes, this group is exceptional in that their cells also may have well-defined MTOCs. In liverworts, mitotic spindle poles arise from acentriolar spherical structures described as polar organizers or centrosomes (Brown and Lemmon, 1990), and this mitotic apparatus is considered to be a transitional state between green algae and seed plants (Brown and Lemmon, 1993). In many bryophytes, meiosis and sometimes mitosis as well occur in cells that contain a single plastid (Shimamura et al., 2003). Like the centrosome, the plastid divides and migrates before nuclear division. Microtubules radiating from the plastid surface function in plastid partitioning, and plastids concomitantly serve as MTOCs of the mitotic and meiotic apparatus (Brown and Lemmon, 1997). Microtubules emanating from the plastid envelope have been shown by transmission electron microscopy (Brown and Lemmon, 1982, 1987), and importantly, experimental studies using microtubule-depolymerizing drugs demonstrated microtubule regrowth from the plastids (Busby and Gunning, 1989), one of few cases in plants in which microtubule polymerization occurred other than at the nuclear envelope. In spermatogenous cells of bryophytes, centriolar centrosomes arise de novo and serve as spindle MTOCs (Robbins, 1984; Vaughn and Renzaglia, 1998). However, there is no information regarding γ-tubulin distribution in these unique microtubule systems. Analysis of γ-tubulin distribution in bryophytes could be expected to provide evidence to increase of understanding of the evolutionary changes in MTOC localization and function postulated to have occurred during plant evolution.

A large number of plant γ-tubulin cDNAs and genes have been cloned and sequenced (Ovenchkina and Oakley, 2001). However, beyond the seed plants, γ-tubulin cDNA has been sequenced in only two species, the moss *Physcomitrella patens* and the fern *Anemia phyllitidis* (Fuchs et al., 1993). In the present study, we isolated and characterized a genomic clone encoding γ-tubulin from a liverwort (Bryophyta), *Conocephalum japonicum*, and compared the sequences among land plant γ-tubulin. We then used the G9 anti-γ-tubulin antibody to thoroughly document the distribution and localization of γ-tubulin in diverse MTOCs in bryophytes.

RESULTS

Analysis of the Gene Encoding γ-Tubulin from a Liverwort and a Comparison of γ-Tubulin Amino Acid Sequences

First, we identified the γ-tubulin gene from the liverwort *Conocephalum japonicum*. To access the genomic information, we designed oligonucleotide primers that corresponded to the conserved sequences of known conventional γ-tubulins. PCR amplification was performed using these primers and *C. japonicum* genomic DNA. The determined nucleotide sequence was used to design PCR primers to isolate the entire genomic DNA of the γ-tubulin gene by means of the vector-annealing PCR method. Sequencing of both strands of the PCR fragments revealed that the γ-tubulin of *C. japonicum* was encoded by a gene encompassing 3582 bp and was intervened by 10 introns. Connecting 11 exons revealed that there was an open reading frame of 1428 bp that encoded a protein of 475 amino acid residues. Throughout the process of γ-tubulin gene identification, we encountered no evidence, such as amplification of genomic fragment of more than one size or obvious sequence polymorphism among the isolated clones after vector-annealing PCR amplification, of the presence of more than one γ-tubulin gene in the haploid genome of *C. japonicum*. We further explored the possibility of the presence of homologous genes by DNA gel blot hybridization. *C. japonicum* genomic DNA was digested with restriction enzymes and probed with a DNA probe of the moss γ-tubulin. Only the bands of expected sizes from the sequences of isolated genes were detected (data not shown). These data indicate that there are no other genes homologous with γ-tubulin in *C. japonicum*. Thus, we conclude that our data are most consistent if there is only one γ-tubulin gene in the *C. japonicum* genome, as is the case with other lower land plants, such as the fern *A. phyllitidis* (Fuchs et al., 1993) and the moss *P. patens*.

We compared the deduced amino acid sequence of *C. japonicum* γ-tubulin with the sequences of other known γ-tubulins. First, it was immediately apparent that *C. japonicum* γ-tubulin belonged to the conventional group of γ-tubulins, because it shared at least 67.5% amino acid identity with other known conventional γ-tubulins. On the other hand, *C. japonicum* γ-tubulin was 39% identical to the *Saccharomyces cerevisiae* γ-tubulin–like protein Tub4p, one of the unconventional γ-tubulins. The γ-tubulin gene product is highly conserved among land plants (Figure 1). The results of our amino acid comparison among plant γ-tubulins is shown in Figure 1B. The *C. japonicum* γ-tubulin showed 89.2 to 97.7% amino acid identity to those of other land plants (*P. patens*, 97.7%; *A. phyllitidis*, 96.4%; Arabidopsis, 90.1%; rice, 89.9%; tobacco, 89.2%; maize, 91.0%). The amino acid identity of *C. japonicum* γ-tubulin was 74.7% to that of *Chlamydomonas reinhardtii* and 69.3% to that of the fission yeast *Schizosaccharomyces pombe*.

G9 Anti-γ-Tubulin Antibody and a 55-kD Peptide of Bryophytes

We used the monoclonal anti-γ-tubulin antibody G9, which was raised against *S. pombe* γ-tubulin (Horio et al., 1999), to detect

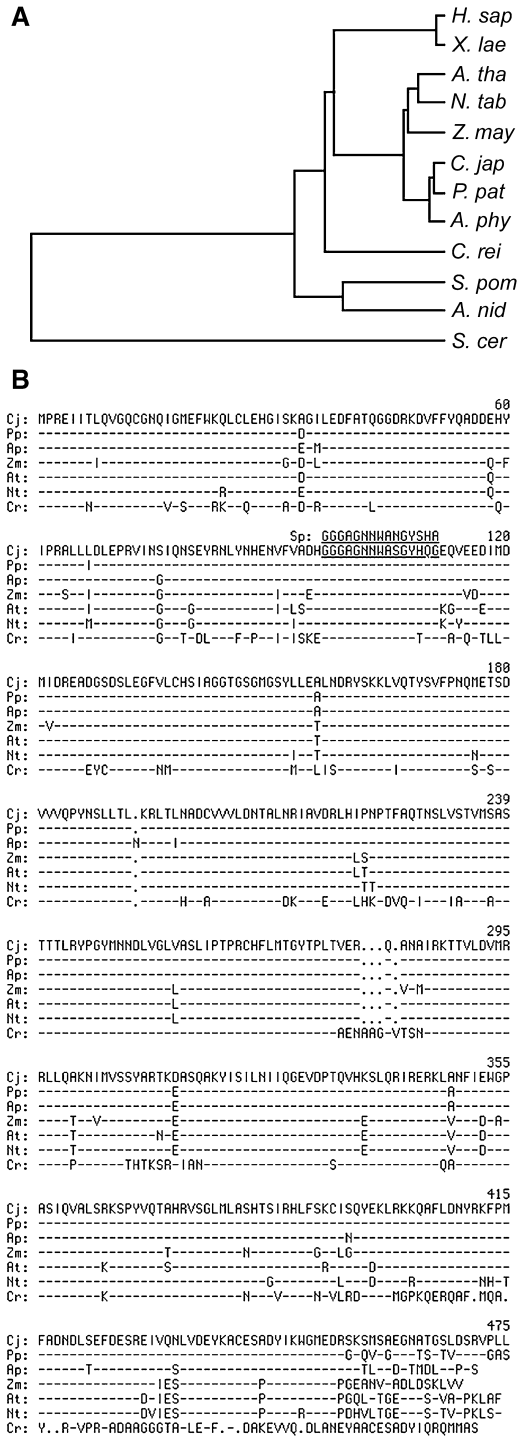

Figure 1. Characterization of the γ-Tubulin Genes of Basal Land Plants.

(A) Deduced phylogeny tree generated by the unweighted pair group method with arithmetic mean algorithm. The γ-tubulins used to generate the tree are listed in **(B)**.

(B) Amino acid sequence comparison of the *C. japonicum* and other plant γ-tubulins. The deduced amino acid sequence of the *C. japonicum* γ-tubulin is shown in the top row. Amino acid sequences of plant γ-tubulins were aligned, and amino acids identical to those of the *C. japonicum* γ-tubulin are indicated by dashes. Dots indicate gaps introduced for the alignment. The inferred recognition epitope of the G9 antibody is underlined.

H. sap, *Homo sapiens*; *X. lae*, *Xenopus laevis*; *A. tha* (At), *Arabidopsis thaliana*; *N. tab* (Nt), *Nicotiana tabacum*; *Z. may* (Zm), *Zea mays*; *C. jap* (Cj), *Conocephalum japonicum*; *P. pat* (Pp), *Physcomitrella patens*; *A. phy* (Ap), *Anemia phyllitidis*; *C. rei* (Cr), *Chlamydomonas reinhardtii*; *S. pom* (Sp), *Schizosaccharomyces pombe*; *A. nid*, *Aspergillus nidulans*; *S. cer*, *Saccharomyces cerevisiae*.

γ-tubulin homologs in various species of bryophytes. The epitope detected by the G9 antibody has been studied and narrowed down to amino acid residues 97 to 111 of *S. pombe* γ-tubulin (GGGAGNNWANGYSHA; our unpublished data). This region is almost completely conserved among known plant γ-tubulins (Figure 1B, underlined) and is fairly well conserved in *S. pombe* γ-tubulin (11 of 15 amino residues are identical). In immunoblots of extracts from sporophytes of *C. japonicum*, it was determined that the G9 antibody did not recognize α- or β-tubulins (Figure 2A, lanes 3 and 4) but clearly cross-reacted with a single band at ~55 kD (Figure 2A, lane 5). The estimated molecular mass of the predicted γ-tubulin protein of *C. japonicum* is 53,359 D. Similar results were obtained in extracts of sporophytes from another bryophyte, *Dumortiera hirsuta* (Figure 2B). G9 has been used successfully for immunofluorescence staining of seed plants (Ovenchkina and Oakley, 2001). The γ-tubulin of Arabidopsis expressed in the fission yeast *S. pombe* has been detected by immunoblot analysis and immunofluorescence staining using G9 (our unpublished data). These facts indicated that the epitope detected by G9 in a variety of bryophytes most likely is γ-tubulin.

Subcellular Localization of G9 Anti-γ-Tubulin Cross-Reactive Materials in Various MTOC Sites in Bryophytes

Bryophytes are known to have a variety of unique MTOCs, such as the plastid surface in quadripolar microtubule systems (QMSs) of meiotic cells (Brown and Lemmon, 1997), centriolar spindle poles in cells undergoing spermatogenesis (Vaughn and Renzaglia, 1998), polar organizers (POs) of mitotic spindles of marchantialean liverworts (Brown and Lemmon, 1990, 1992), and radial microtubule systems (RMSs) during meiosis in *C. japonicum* (Brown and Lemmon, 1988; Shimamura et al., 1998). Except for the RMS, these MTOCs have never been seen in seed plants. Reproductive cells generally lack distinctive cortical microtubule systems. To ascertain the occurrence of γ-tubulin in these MTOC sites, we examined the localization of G9 anti-γ-tubulin cross-reactive materials in putative MTOCs in bryophytes

QMS in Moss Meiosis

The sporocytes of bryophytes typically have a single plastid. In prophase I, the single plastid divides into four plastids before nuclear division. The positioning of the four plastids at the tetrad poles is associated with a QMS and the formation of an unusual quadripolar spindle (Brown and Lemmon, 1997). In

prophase I sporocytes of the moss *Entodon seductrix*, microtubules emanate from individual plastids and interact to form a QMS (Figure 3A). G9 anti-γ-tubulin cross-reactive materials are distributed around the surfaces of the four plastids as numerous punctae (Figure 3B, arrowheads).

Centriolar MTOCs in Mitosis of Spermatogenous Cells

In spermatogenous cells of bryophytes, bicentrioles arise de novo in MTOCs just outside the nuclear envelope. Once formed, bicentrioles and associated pericentriolar material separate for the final mitosis of spermatogenous division (Vaughn and Renzaglia, 1998). Figures 3D to 3F show the cell just before the final spermatogenous cell division in the liverwort *Makinoa crispata*. Two distinctive fluorescent dots of the γ-tubulin homolog in Figure 3E are in the position of the centriolar centrosomes.

POs and Metaphase Spindles in Archesporial Mitosis of Marchantia polymorpha

During mitosis in polyplastidic cells of marchantialean liverworts, plastids do not serve as MTOCs. Instead, POs, which arise de novo outside of the nuclear envelope, are the foci of a prophase spindle (Brown and Lemmon, 1992). During archesporial mitosis in *Marchantia polymorpha*, prophase spindles focus on discrete POs (Figure 3G). Distinctive dots of G9 anti-γ-tubulin cross-reactive materials (Figure 3H) correspond to POs. There was no colocalization of microtubules and γ-tubulin homolog (cf. Figures 3G and 3H). As the metaphase spindle develops, POs of *M. polymorpha* disappear and spindle poles disperse (Figure 3J). The G9 staining pattern in the metaphase spindle is more diffuse than that in prophase, but it is clearly restricted to the pole regions (Figure 3K).

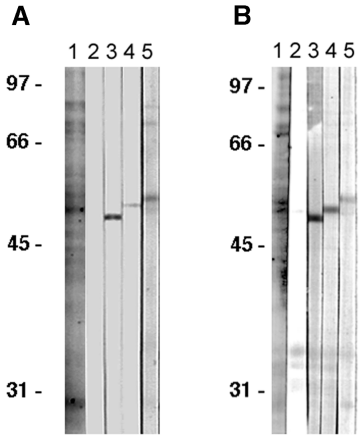

Figure 2. Immunoblot Analysis of G9 Antibody in Protein Extracts from Sporogenous Tissue of the Bryophytes *C. japonicum* and *D. hirsuta*.

(A) *C. japonicum*.
(B) *D. hirsuta*.
Lane 1, Coomassie brilliant blue staining; lane 2, control immunoblot without primary antibodies; lanes 3 and 4, monoclonal antibodies against α- and β-tubulin, respectively; lane 5, G9 anti-γ-tubulin. The positions of molecular mass markers and their molecular masses (kD) are indicated at left.

Spindles, RMSs, and Phragmoplasts during Meiosis in Conocephalum

Members of the genus *Conocephalum* (Marchantiidae) have some unique microtubule systems during meiosis (Brown and Lemmon, 1988; Shimamura et al., 1998). Metaphase spindles are barrel shaped with broad poles that never converge into foci. Thus, the spindle microtubules are oriented parallel to each other and deliver the chromosomes to broad truncated poles. G9 anti-γ-tubulin cross-reactive materials localized along microtubules of the mature spindle, but with the distribution clearly biased toward the spindle poles (Figure 3N). After the second round of meiosis, simultaneous cytokinesis partitioned the elongate sporocyte into a linear tetrad. RMSs emanating from telophase nuclei are an important feature of the cytokinetic apparatus during meiosis in *Conocephalum*, ensuring the equal distribution of cytoplasm and the positioning of phragmoplasts. G9 anti-γ-tubulin cross-reactive materials were conspicuous both at nuclear surfaces at the sites of putative MTOCs of the RMS and in phragmoplasts (Figure 3P). The unstained midzone where the cell plate is deposited was more conspicuous when stained for γ-tubulin homologs (Figure 3P, arrowheads) than for microtubules (Figure 3O).

Change in the Localization of G9 Anti-γ-Tubulin Cross-Reactive Materials during the Monoplastidic Meiotic MTOC Cycle in *D. hirsuta*

In monoplastidic bryophytes, meiotic MTOCs change in form and position during the cell cycle (Brown and Lemmon, 1997) from the plastid surface (prophase I and II) to the spindle pole region (metaphase I and II) to the nuclear surface and phragmoplasts (telophase I and II) (see Figure 10). Because meiotic cells of *D. hirsuta* are relatively large (~30 μm) with easily recognized MTOC sites, further studies of the distribution of G9 anti-γ-tubulin cross-reactive materials were performed with this material. The microtubule and plastid distribution during meiosis in *D. hirsuta* have been described (Shimamura et al., 2000, 2001).

Premeiotic Plastid Division and Partitioning

In premeiotic interphase, a reticulate array of microtubules spanned the cytoplasm. Dots of G9 anti-γ-tubulin cross-reactive materials were distributed randomly in the cytoplasm (Figure 4B). In plastid division during prophase, microtubules emanated from dividing plastids (Figures 4C and 4E). G9 anti-γ-tubulin cross-reactive materials were localized around the dividing plastids (Figures 4D and 4F). Optical sections by confocal laser scanning microscopy demonstrated different localization of γ-tubulin homologs and microtubules. Although a portion of γ-tubulin homolog seemed to localize along microtubules, the majority of γ-tubulin homolog occurred at the plastid surface (Figures 4G and 4H). In controls in which the primary antibody (G9) was omitted, plastids were unstained (Figures 4I

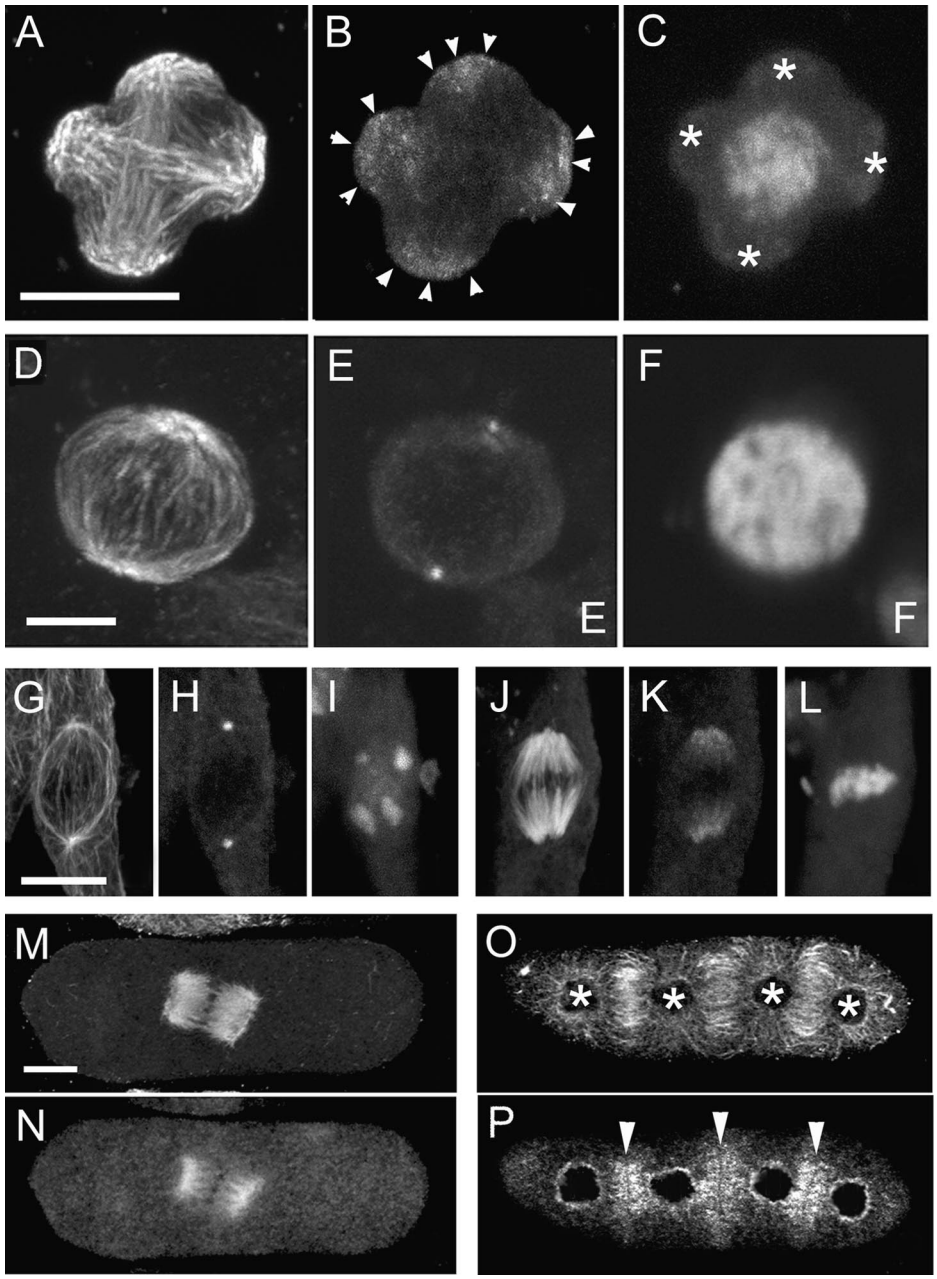

Figure 3. Triple Labeling for γ-Tubulin, α and β-Tubulin, and DNA Shows the Subcellular Localization of γ-Tubulin Homologs in Some Typical MTOC Sites in Bryophytes.

(A) to **(C)** A QMS during meiotic prophase of the moss *Entodon seductrix*. Note that γ-tubulin homologs **(B)** are localized around the four daughter plastids (arrowheads in **[B]** and asterisks in **[C]**) from which microtubules emanate **(A)**.
(D) to **(F)** A prophase spindle with centrioles in the final spermatogenous mitotic division of the liverwort *Makinoa crispate*. Two distinctive fluorescent dots **(E)** at two distinctive MTOCs **(D)** are considered to be equivalent to centriolar centrosomes.
(G) to **(L)** A prophase spindle with POs (**[G]** to **[I]**) and a metaphase spindle with broad poles (**[J]** to **[L]**) during archesporial mitosis of the liverwort *Marchantia polymorpha*. Note that although a prophase spindle arises from the discrete POs where γ-tubulin homologs locate **(H)**, the polar distribution of γ-tubulin extending along proximal portions is seen in a metaphase spindle that has dispersed MTOCs **(K)**.
(**M)** to **(P)** A barrel-shaped metaphase spindle in meiosis I (**[M]** and **[N]**) and RMSs and phragmoplasts in meiotic telophase II (**[O]** and **[P]**) of the liverwort *C. japonicum*. Note that γ-tubulin homologs localized on the mature spindle microtubules, but distribution clearly was biased toward the broad spindle poles **(N)**. RMSs emanating from telophase nuclei (asterisks in **[O]**) and phragmoplasts develop between nuclei. γ-Tubulin homologs localized at putative MTOCs, the nuclear surface, and phragmoplasts **(P)**. Arrowheads in **(P)** show three newly forming cell plates that appear as dark, unstained lines.
Microtubules (**[A]**, **[D]**, **[G]**, **[J]**, **[M]**, and **[O]**), γ-tubulin homologs (**[B]**, **[E]**, **[H]**, **[K]**, **[N]**, and **[P]**), and nuclei (**[C]**, **[F]**, **[I]**, and **[L]**) were stained using anti-plant-tubulin, G9 anti-γ-tubulin, and 4′,6-diamidino-2-phenylindole (DAPI), respectively. Bars = 10 μm.

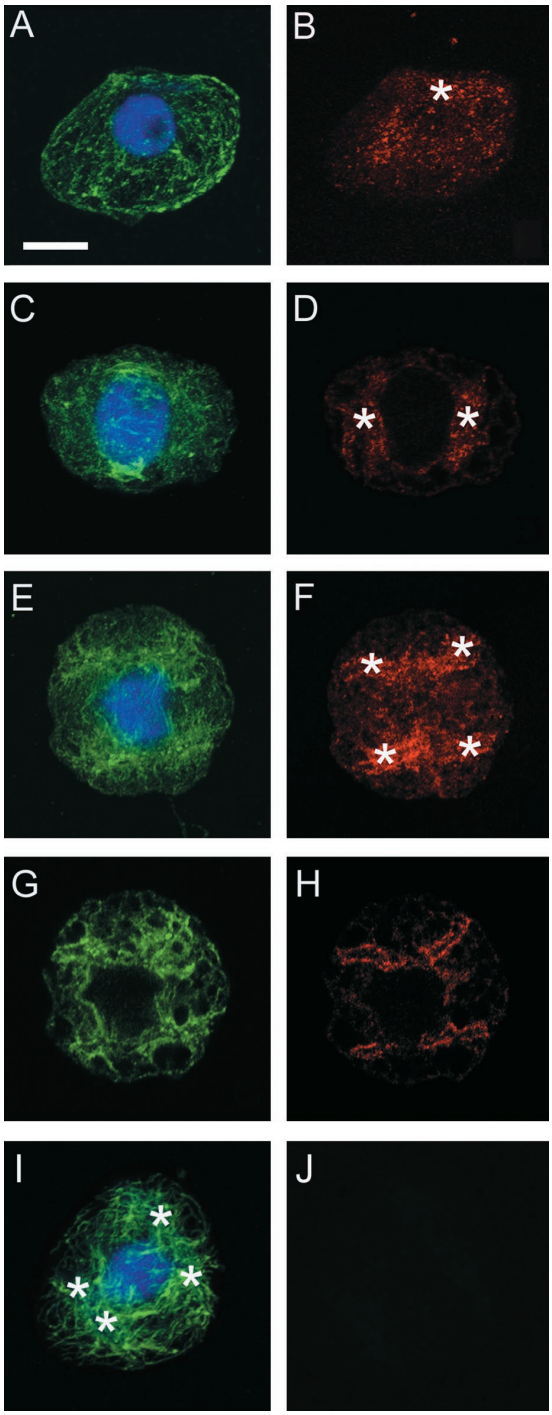

Figure 4. Changes in the Subcellular Localization of γ-Tubulin Homologs during Plastid Division and Partitioning in Monoplastidic Meiosis of *D. hirsuta* (Premeiotic Interphase to Prophase I).

(**A**) and **(B)** A premeiotic interphase cell with a single plastid (asterisk in **[B]**). Note that dots of γ-tubulin homologs are distributed randomly in the cytoplasm **(B)** with reticular arrays of microtubules **(A)**.
(C) and **(D)** An early prophase cell with two daughter plastids (asterisks in **[D]**). Note the γ-tubulin homologs localized around the two plastids.
(E) to **(H)** A mid-prophase cell with four daughter plastids (asterisks in **[F]**). Note that the localization of γ-tubulin homologs around the four daughter plastids becomes more prominent. **(G)** and **(H)** show single optical sections of **(E)** and **(F)**, respectively.
(I) and **(J)** A mid-prophase cell with four daughter plastids (asterisks in **[I]**). The primary antibody (G9) is omitted (a similar stage is shown in **[E]**). Crosstalk and nonspecific signal of secondary antibody were not observed.
Microtubules (green signal in **[A]**, **[C]**, **[E]**, **[G]**, and **[I]**), DNA (blue signal in **[A]**, **[C]**, **[E]**, **[G]**, and **[I]**), and γ-tubulin homologs (red signal in **[B]**, **[D]**, **[F]**, **[H]**, and **[J]**) were stained using anti-plant-tubulin, DAPI, and G9 anti-γ-tubulin, respectively. **(A)** and **(B)**, **(C)** and **(D)**, **(E)** and **(F)**, **(G)** and **(H)**, and **(I)** and **(J)** show the same cells with different color combinations. Bar = 10 μm.

and 4J). Autofluorescence of plastids was removed completely through the process of detergent extraction (see Methods).

Meiosis I

In late prophase I, G9 anti-γ-tubulin cross-reactive materials disappeared from the plastid surface and appeared at spindle poles on the tips of the distorted nucleus as distinct fluorescent dots. Contrary to the localization of γ-tubulin homologs, a subset of several microtubules emanated from the plastids in addition to the spindle microtubules. Translocation of γ-tubulin homolog seemed to precede the reorganization of microtubules into the spindle (Figures 5A and 5B). Distinct spots marked the polar regions of the forming spindle. In meiosis I, G9 anti-γ-tubulin cross-reactive materials were localized conspicuously at polar regions of the spindle during metaphase (Figures 5C and 5D) and anaphase (Figure 5F, arrowheads). In telophase I, two microtubule systems appeared: the radial microtubules, which emanated from the nuclear surfaces, and the phragmoplasts. As shown in previous studies of *Conocephalum* (Brown and Lemmon, 1988; Shimamura et al., 1998), the first division phragmoplast was very well developed but incompetent to deposit a cell plate. G9 anti-γ-tubulin cross-reactive materials were detected both in phragmoplasts and on the nuclear surface but were clearly absent from the plastid surfaces (Figures 5G and 5H).

Meiosis II

Because phragmoplasts in telophase I disappeared without completing new cell walls, a binucleated cell was formed. In prophase II, microtubules emanating from plastids surrounded prophase nuclei (Figure 6A). Punctate staining of G9 anti-γ-tubulin cross-reactive materials reappeared on the plastid surfaces (Figure 6B). Developmental features of metaphase II spindles were identical to those of the metaphase I spindle. G9 anti-γ-tubulin cross-reactive materials were localized in the polar regions of metaphase II spindles (Figures 6C and 6D). During telophase II, radial microtubules once again emanated from the surfaces of the four nuclei, and phragmoplasts reassembled between all sister nuclei (Figures 6E and 6F). At this stage, γ-tubulin homologs were detected in phragmoplasts and on the nuclear surfaces. Optical sections clearly show the localiza-

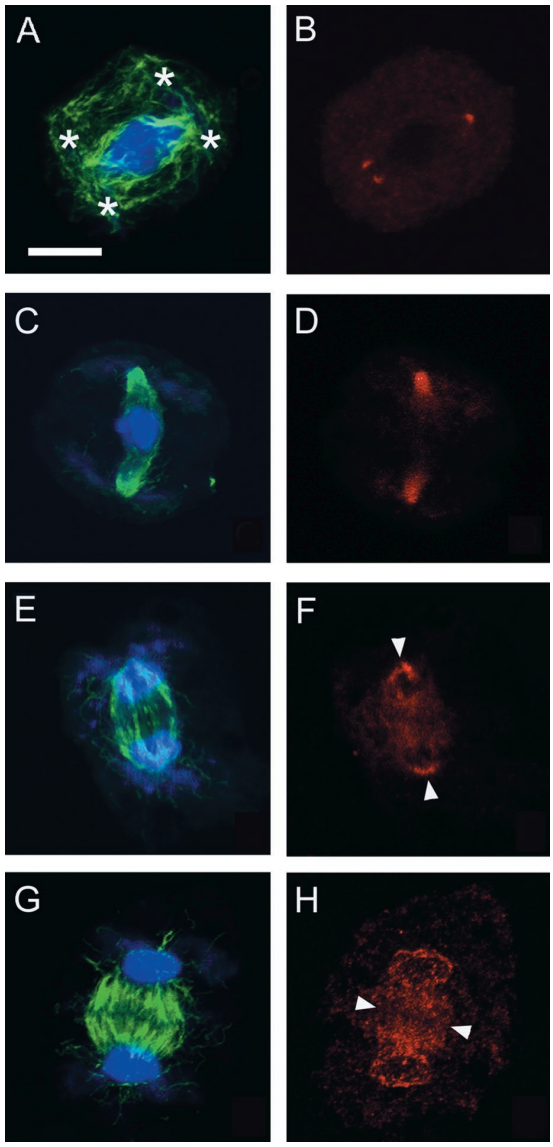

Figure 5. Changes in the Subcellular Localization of γ-Tubulin Homologs during the Progression of Meiosis I in Monoplastidic Cells of *D. hirsuta* (Prometaphase to Anaphase I).

(A) and **(B)** A prometaphase cell with four daughter plastids (asterisks in **[A]**). Note that the γ-tubulin localizes distinctly near the spindle poles.
(C) and **(D)** A cell in metaphase I. Note that γ-tubulin homologs are localized along spindle microtubule arrays but are absent from the kinetochore side.
(E) and **(F)** A cell in anaphase I. γ-Tubulin homologs are localized at the polar surface of each daughter nucleus (arrowheads in **[F]**).
(G) and **(H)** A cell in telophase I. γ-Tubulin homologs are localized both in phragmoplasts and on the nuclear surface. The position of the cell plate is shown by arrowheads.
Microtubules (green signal in **[A]**, **[C]**, **[E]**, and **[G]**), DNA (blue signal in **[A]**, **[C]**, **[E]**, and **[G]**), and γ-tubulin homologs (red signal in **[B]**, **[D]**, **[F]**, and **[H]**) were stained using anti-plant-tubulin, DAPI, and G9 anti-γ-tubulin, respectively. **(A)** and **(B)**, **(C)** and **(D)**, **(E)** and **(F)**, and **(G)** and **(H)** show the same cells with different color combinations. Bar = 10 μm.

tion of γ-tubulin homologs at presumptive MTOC sites on the nuclear surface, and there was no signal from within the nucleus (Figures 6G and 6H).

Distribution of G9 Anti-γ-Tubulin Cross-Reactive Materials on Isolated Plastids and Nuclei

Because immunofluorescence observations strongly suggested that γ-tubulin is associated with organelles during meiosis, an attempt was made to confirm the localization of G9 cross-reactive materials on isolated organelles from meiotic sporocytes of *D. hirsuta*. Isolated intact plastids and nuclei were distinguished from other organelles by size, shape, and DNA staining patterns (Figures 7A, 7B, 7D, and 7E). Less than 50% of isolated plastids and nuclei had γ-tubulin homologs at their surfaces, as indicated by immunofluorescence (Figures 7C and 7F). Microtubule-initiating activity from the surfaces of isolated organelles was investigated. When incubated with rhodamine-labeled tubulin purified from animal sources, unfixed isolated plastids (Figures 7G and 7H) were able to nucleate microtubules at their surfaces. Such microtubules may obtain a length of 10 to 20 μm (Figures 7I and 7J).

Distribution of G9 Anti-γ-Tubulin Cross-Reactive Materials after Treatment with the Anti-Microtubule Drug Oryzalin

To test whether the specific localization of γ-tubulin homologs in MTOC sites was affected by the disorganization of the microtubule system, sporocytes of *D. hirsuta* in meiotic stages were treated with oryzalin solution for 20 min and examined using anti-microtubule and G9 anti-γ-tubulin immunocytochemistry. Solutions of ≥5 μM oryzalin caused drastic microtubule disorganization. Microtubules emanating from plastids were more sensitive to the treatment than were spindle fibers and RMSs (Figure 8A). Cells treated with 20 μM oryzalin contained no microtubules other than some remnants of spindle fibers and RMSs (Figures 8A, 8C, and 8E). Although it was not as prominent as in control cells, G9 anti-γ-tubulin cross-reactive materials were detectable on or near the prophase plastid surface (Figure 8B, asterisks) when microtubules were disrupted by oryzalin. Spindle microtubules seemed to be most resistant to disorganization. In metaphase cells, the distribution of G9 anti-γ-tubulin cross-reactive materials was restricted along the remnant microtubules of spindle fibers (Figures 8C and 8D). The localization of γ-tubulin homologs on the telophase nuclear surface was not affected by treatment with oryzalin (Figures 8E and 8F). There was no colocalization of γ-tubulin homologs and microtubule remnants of RMSs (Figure 8E, arrowheads). Longer oryzalin treatments (2 h) did not affect the localization of G9 anti-γ-tubulin cross-reactive materials around the plastids (Figures 8G and 8H).

DISCUSSION

The γ-Tubulin Gene Is Conserved in Land Plants

The present study shows that the γ-tubulin gene of *C. japonicum* most likely is present as a single-copy gene in the ge-

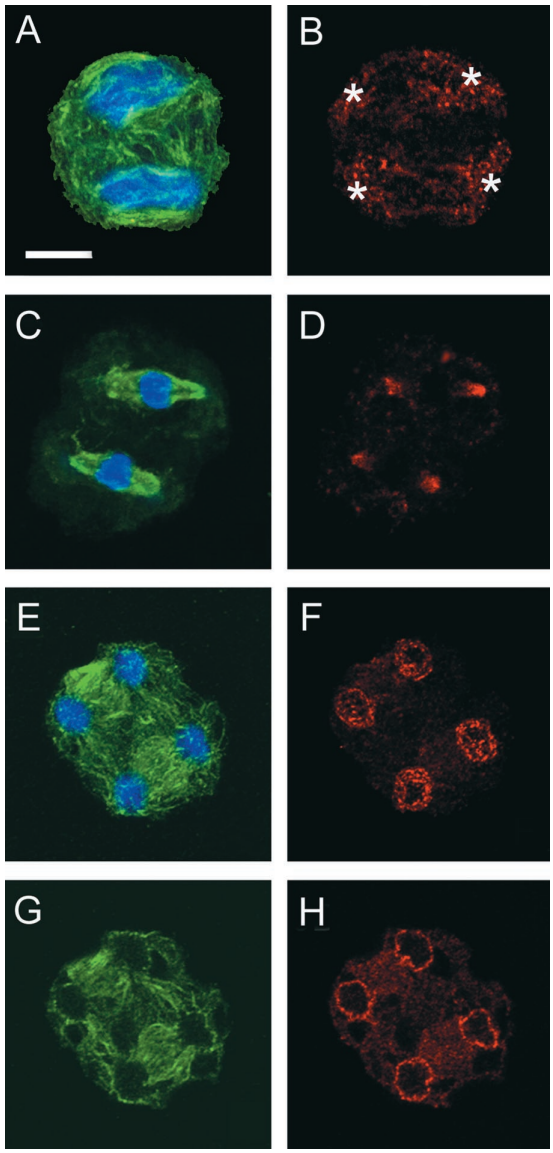

Figure 6. Changes in the Subcellular Localization of γ-Tubulin Homologs during the Progression of Meiosis II in Monoplastidic Cells of *D. hirsuta* (Prophase II to Telophase II).

(A) and **(B)** A cell in prophase II. Note the reappearance of the localization of γ-tubulin homologs around the plastids (asterisks in **[B]**).
(C) and **(D)** A cell in metaphase II. The broad localization of γ-tubulin homologs in the polar region of spindles is identical to that in prophase I.
(E) to **(H)** A cell in telophase II. Note that γ-tubulin homologs are localized at the nuclear surface and early phragmoplasts are localized between daughter nuclei. **(G)** and **(H)** show single optical sections of **(E)** and **(F)**, respectively.
Microtubules (green signal in **[A]**, **[C]**, **[E]**, and **[G]**), DNA (blue signal in **[A]**, **[C]**, **[E]**, and **[G]**), and γ-tubulin homologs (red signal in **[B]**, **[D]**, **[F]**, and **[H]**) were stained using anti-plant-tubulin, DAPI, and G9 anti-γ-tubulin, respectively. **(A)** and **(B)**, **(C)** and **(D)**, **(E)** and **(F)**, and **(G)** and **(H)** show the same cells with different color combinations. Bar = 10 μm.

nome, as it is in other lower land plants. The γ-tubulin gene was found as a single-copy gene in the fern *A. phyllitidis* (Fuchs et al., 1993), the moss *P. patens*, and the green alga *C. reinhardtii* (Silflow et al., 1999). Duplication of the γ-tubulin gene may have occurred through the evolution of land plants; at least two γ-tubulin genes are recognized in seed plants such as Arabidopsis (Liu et al., 1994) and maize (Ovenchkina and Oakley, 2001). A phylogenetic analysis of predicted protein sequences

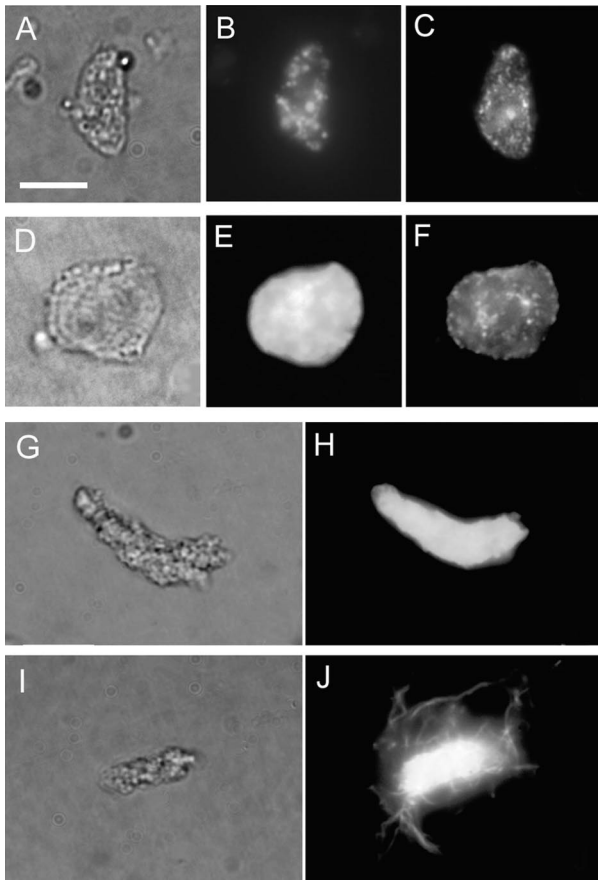

Figure 7. Localization of γ-Tubulin Homologs in Isolated Organelles, and Microtubule-Initiating Activity of Isolated Plastids from Sporocytes of *D. hirsuta*.

(A) to **(C)** An isolated plastid. γ-Tubulin homologs are localized on the plastid surface.
(D) to **(F)** An isolated nucleus. γ-Tubulin homologs are localized on the nuclear surface.
DNA (**[B]** and **[E]**) and γ-tubulin homologs (**[C]** and **[F]**) were stained using DAPI and G9 anti-γ-tubulin. **(A)** and **(D)** show differential interference contrast views. **(A)** to **(C)** and **(D)** to **(F)** show the same cells.
(G) and **(H)** Unfixed isolated plastid just after isolation.
(I) and **(J)** Isolated plastid after incubation with rhodamine-labeled tubulin. Rhodamine-labeled tubulin nucleates from the plastid.
(G) and **(I)** show differential interference contrast views of the same plastids in **(H)** and **(J)**, respectively. **(H)** and **(J)** show views through a red filter to detect the rhodamine signal. Chlorophyll autofluorescence also is seen in these images. Bar = 10 μm.

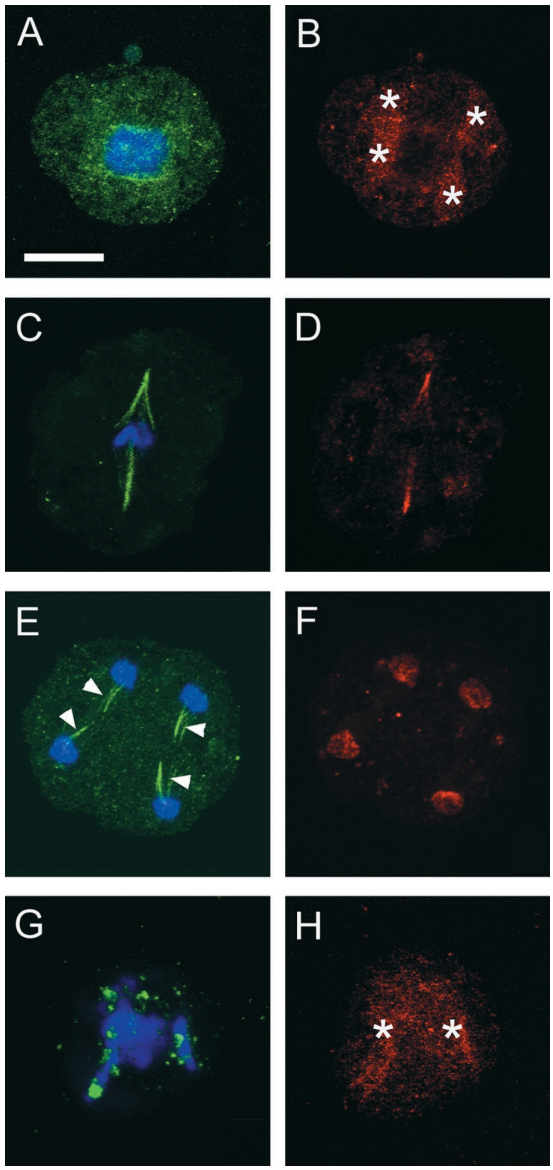

Figure 8. Effects of the Anti-Microtubule Drug Oryzalin on the Subcellular Localization of γ-Tubulin Homologs in Monoplastidic Cells of *D. hirsuta*.

(A) and **(B)** A prophase I cell treated for 20 min with 20 μM oryzalin. Plastid-based microtubules are absent **(A)**. Note that γ-tubulin homologs are detected around the plastids **(B)**.

(C) and **(D)** A metaphase I cell treated for 20 min with 20 μM oryzalin. γ-Tubulin homologs are localized along the remnant microtubule bundles.

(E) and **(F)** A telophase II cell treated for 20 min with 20 μM oryzalin. Note that no γ-tubulin homologs are localized along the remnant microtubules of RMS. Oryzalin treatment did not affect the γ-tubulin homolog localization on the nuclear surface.

(G) and **(H)** An early meiotic cell treated for 2 h with 20 μM oryzalin. Note that γ-tubulin homologs still remain around the plastids (asterisks in **[H]**).

Microtubules (green signal in **[A]**, **[C]**, **[E]**, and **[G]**), DNA (blue signal in **[A]**, **[C]**, **[E]**, and **[G]**), and γ-tubulin homologs (red signal in **[B]**, **[D]**, **[F]**, and **[H]**) were stained using anti-plant-tubulin, DAPI, and G9 anti-γ-tubulin, respectively. **(A)** and **(B)**, **(C)** and **(D)**, **(E)** and **(F)**, and **(G)** and **(H)** show the same cells with different color combinations. Bar = 10 μm.

revealed monophyly with two distinctive branches of land plants (Figure 1A). The occurrence of two groups with regard to γ-tubulin (angiosperms and nonflowering plants) might reflect the presence or absence of centrosomes in the life cycle. Among the extant seed plants (Spermatophyta), only ginkgo and cycads have flagellated spermatozoids and produce centrioles de novo. Neither has been studied molecularly. Nine of the 10 introns of the *C. japonicum* γ-tubulin gene occurred at the same sites as the nine introns of the Arabidopsis γ-tubulin genes. The predicted amino acid sequence of the *C. japonicum* γ-tubulin protein is 89.2 to 97.7% identical to those of other γ-tubulins of land plants. These results suggests that both the structure and the predicted protein of the γ-tubulin gene are highly conserved in land plants.

γ-Tubulin Characterizes Diverse MTOCs in Bryophytes

The G9 antibody specifically recognizes γ-tubulin in immunoblots of protein extracts and in immunohistochemistry of bryophytes as well as in a wide variety of other organisms (Ovenchkina and Oakley, 2001; Horio et al., 2002). Using this antibody, we demonstrated that γ-tubulin characterizes the putative MTOC sites of bryophytes, such as centriolar MTOCs (Figures 3E and 9A), discrete MTOCs without centrioles (Figures 3H and 9B), diffuse MTOCs similar to those in seed plants (Figures 3K, 3N, 3P, 5D, 5F, 5H, 6D, 6F, 6H, 9D, 10E, 10F, and 10H), and membrane-associated MTOCs (Figures 3B, 3P, 4D, 4F, 4H, 5H, 6B, 6F, 6H, 9C, 10B, 10C, 10F, 10G, and 10H).

Correlation of the γ-Tubulin Localization Pattern with the MTOC Cycle

We were able to provide details on the changes in location of γ-tubulin during the meiotic cycle in the large monoplastidic sporocytes of the liverwort *D. hirsuta*. We expected that the cell cycle–dependent distribution patterns of γ-tubulin (Figure 10) were common in the MTOC cycle during monoplastidic meiosis of bryophytes based on changing patterns of microtubules during meiosis (Brown and Lemmon, 1997; Shimamura et al., 2001). The mechanism of cell cycle–dependent translocation of γ-tubulin is not clear. This little-understood phenomenon has been reported in algae and animal cells. In the green alga *Boergesenia forbesii*, γ-tubulin was not detected at the centrosome during interphase but began to concentrate at the centrosome from prophase onward (Motomura et al., 2001). In animal cells, in which γ-tubulin always associates with centrosomes throughout the mitotic cycle, the amount of centrosome-associated γ-tubulin nevertheless increases during prophase (Khodjakov and Rieder, 1999).

Plastid-Based MTOCs

In monoplastidic meiosis of bryophytes, it is typical for the single plastid to divide in anticipation of nuclear division and for the spindle apparatus to be organized in association with plastid migration and division (Shimamura et al., 2003). Electron microscopy and immunofluorescence microscopy suggested that microtubules emanate from these plastid envelopes directly or

from discrete bodies of electron-dense materials near the plastids (Brown and Lemmon, 1997). The microtubule-nucleating ability of the plastid-based MTOC has been shown by the recovery of microtubules from anti-microtubule drug treatments in vivo (Busby and Gunning, 1989). The demonstration of γ-tubulin at the periphery of the dividing plastids in the proper position to serve as the MTOC both in vivo and in vitro supports the contention that MTOCs are associated with the plastid envelope in monoplastidic cells.

The cell cycle–dependent location of γ-tubulin at the plastid surface and the nucleation of microtubules from the plastid surface seem to occur concurrently. During meiosis in *D. hirsuta*, peripheral localization of γ-tubulin on plastids was observed in both prophase I (Figure 4) and prophase II (Figure 6B). At other stages of the meiotic cycle, there was no localization of γ-tubulin on the plastid surface. A recent study (Dibbayawan et al., 2001) reported γ-tubulin, but not microtubules, in association with proplastids in wheat root tip cells. Perhaps such an association of γ-tubulin and plastids in seed plants is an evolutionary relic, and this γ-tubulin has lost its function in the organization of spindles that instead resides with γ-tubulin associated with the nuclear envelope. Should the presence of such non-MTOC γ-tubulin prove to be widespread, then additional studies will be needed to search for their possible presence in plants.

The ability of isolated centrosomes and/or nuclei to nucleate microtubules has been demonstrated in various animal and plant cells (Mizuno, 1993; Stoppin et al., 1994; Joshi and Zhou, 2001). Here, we show microtubule-nucleating activity in association with the surface of the isolated plastids in vitro. MTOC activity was restricted to a subpopulation of the plastids isolated from sporocytes in meiosis. Although the in vitro incubation with labeled tubulin and γ-tubulin antibody is important for studying the function of γ-tubulin, it was difficult to determine whether G9 antibody blocks the in vitro nucleation of microtubule from plastids or if plastids isolated from certain developmental stages lack MTOC activity. The elucidation of the role of γ-tubulin in microtubule nucleation from plastids needs further investigation.

POs: γ-Tubulin Localizes in Discrete MTOCs without Centrioles

Our observations clearly show that γ-tubulin is associated exclusively at the discrete POs that organize the mitotic spindle in liverworts. Interestingly, γ-tubulin staining gradually diffused as spindles developed, and the distribution of γ-tubulin in mature metaphase spindles resembled the typical anastral plant spindle. The shape of the plant spindle ranges from fusiform with pointed poles to barrel shaped with broad poles. The broad poles often constitute numerous distinct “minipoles” (Schnepf, 1984) in which subsets of microtubules converge. The change in γ-tubulin position from a close association with discrete POs to the broad polar region of the mature spindle appears to correlate with a cell cycle–dependent migration of the MTOC, as in the case of plastid-based MTOCs.

Spindles and Phragmoplasts: the Diversity of γ-Tubulin Localization in Prophase Spindles Reflects the Evolution of Plant MTOCs

γ-Tubulin localization in various types of prophase spindle poles in bryophytes supports the premise that γ-tubulin is an evolutionarily conserved component of the spindle MTOC in

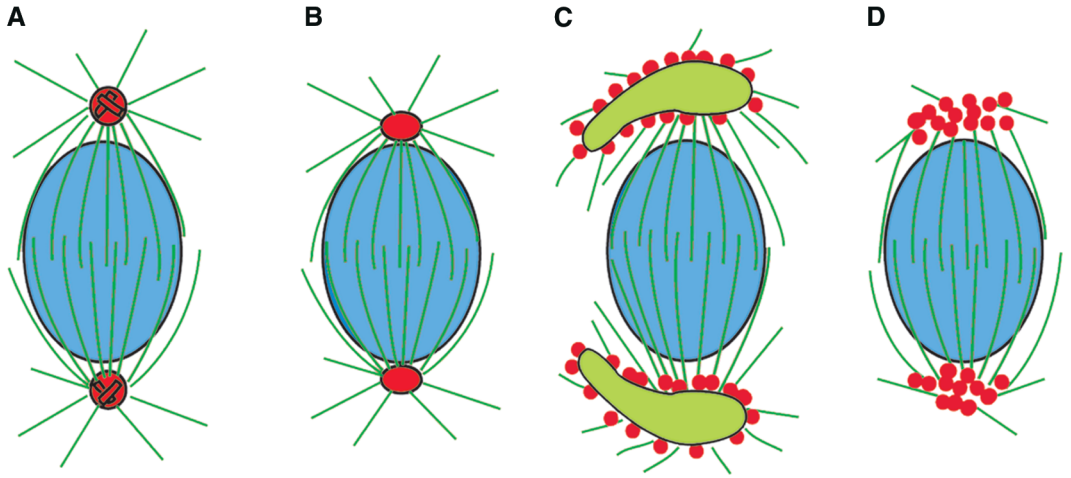

Figure 9. Schemes of the Diversity of γ-Tubulin Localization in Prophase Spindles.

(A) A cell with centrioles. In green algae and in spermatogenous cells of bryophytes, γ-tubulin localizes precisely at centriolar centrosomes.
(B) A cell with POs. γ-Tubulin localizes distinctly at acentriolar POs of some liverworts.
(C) The spindle during monoplastidic meiosis in some bryophytes arises from daughter plastids. γ-Tubulin localizes on the plastid surface.
(D) In higher plants, γ-tubulin localizes indistinctly at polar regions of diffuse spindles.
Microtubules, plastids, nuclei, and γ-tubulin are shown as dark green, lime green, blue, and red, respectively.

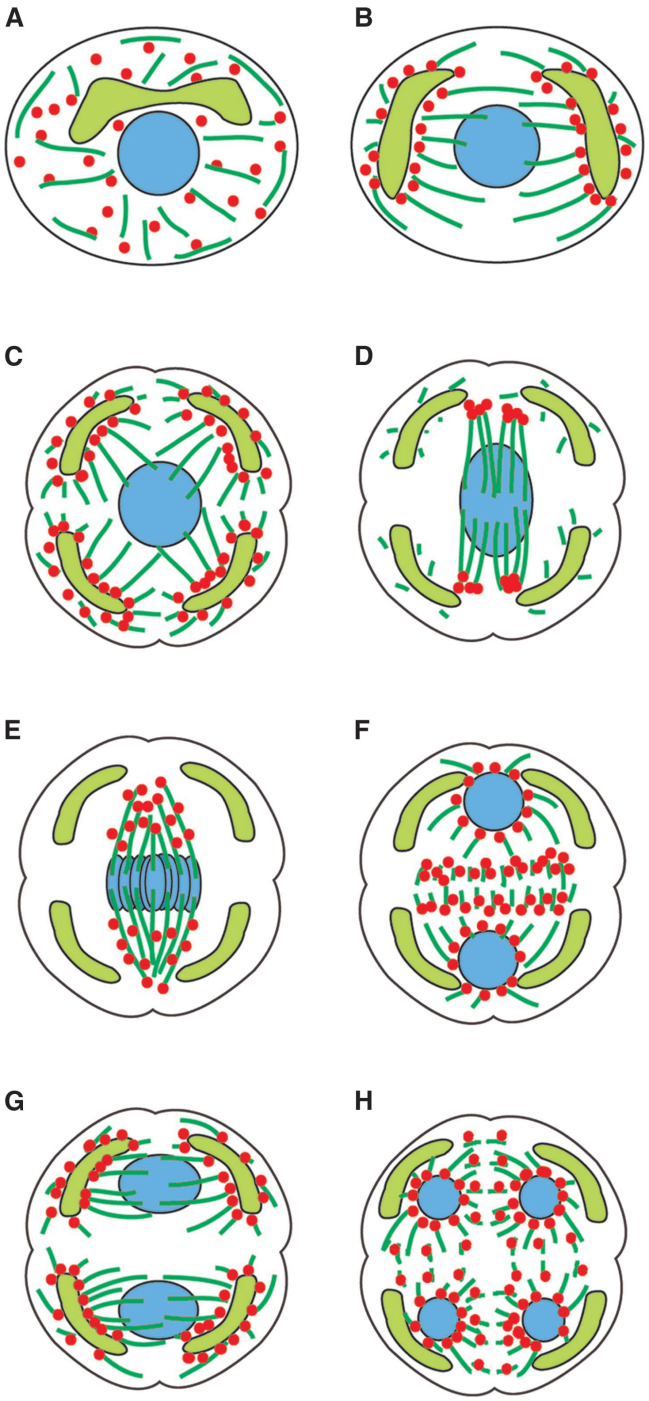

Figure 10. Schemes of the MTOC Cycle during Monoplastidic Meiosis in Bryophytes.

(A) Premeiotic interphase.
(B) Early prophase.
(C) Mid prophase. QMS and cytoplasmic lobing predict the polarity of the two meiotic divisions.
(D) Late prophase.
(E) Metaphase I.
(F) Telophase I.
(G) Early prophase II.
(H) Early telophase II.
Microtubules, plastids, nuclei, and γ-tubulin are shown as dark green, lime green, blue, and red, respectively.

eukaryotes. Figure 9 shows the diversity of prophase spindle formation in plants. γ-Tubulin was distributed conspicuously and specifically at centriolar centrosomes of spermatogenous cells of bryophytes (Figure 9A) and the acentriolar POs of liverworts (Figure 9B). In monoplastidic cells of bryophytes, γ-tubulin was distributed as small dots on the plastid surface (Figure 9C). Although it is difficult to determine the more ancestral character, POs and plastid-based spindles seem to be transitional stages between centriolar spindles of green algae and the diffuse spindles of seed plants. γ-Tubulin localization in various types of prophase spindle poles also may reflect the evolutionary stages of plant spindle development. In higher plants, the diffuse prophase spindle is organized from the perinuclear area. γ-Tubulin localizes indistinctly at the pole region of the diffuse spindles (Figure 9D) (Liu et al., 1993, 1994). Some green algae, which do not produce flagellate zoospores, lack centriolar centrosomes. These spindles are barrel shaped, like those of most land plants (Pickett-Heaps, 1975; Graham and Kaneko, 1991). The loss of motile cells and the multiplication of plastids through the evolution of land plants seem to be related to the change of γ-tubulin localization and the acquisition of diffuse spindle poles. In bryophytes, γ-tubulin is distributed along nearly all metaphase spindles but absent from kinetochores, a situation commonly observed in higher plants (Liu et al., 1993; Joshi and Palevitz, 1996). γ-Tubulin localization along spindle microtubules in the polar region seems to correlate with the establishment of the mature metaphase spindle in land plants.

Cytokinesis in land plants involves cell plate formation directed by the phragmoplast. Although γ-tubulin is widely dispersed in the phragmoplast and appears to colocalize with microtubules, the unstained zone at the cell plate is wider when the γ-tubulin is viewed exclusively, indicating a concentration of γ-tubulin at distal regions of the phragmoplast (Liu et al., 1993, 1995; Joshi and Palevitz, 1996; this study). The structure of bryophyte phragmoplasts and the associated γ-tubulin distribution pattern also are indistinguishable from those of seed plants.

MTOCs on the Nuclear Surface: γ-Tubulin Can Associate with the Nuclear Membrane

In seed plants, there is a general consensus that the nuclear envelope is the principal site of microtubule assembly (Stoppin et al., 1994), and an electron microscopic image that suggests the association of microtubules with the nuclear envelope has been shown (Lambert, 1980). The perinuclear localization of γ-tubulin is evident in prophase nuclei but is faint in telophase nuclei (Liu et al., 1993). Our observations of liverwort meiosis clearly show the opposite; in cytokinesis, γ-tubulin occurred both as distinct dots at the nuclear surface and as diffuse staining throughout the phragmoplast. Furthermore, the association

of γ-tubulin with the nuclear envelope was more distinct during telophase (Figures 5H, 6F, and 6H) than in prophase (Figures 4 and 6B). Although γ-tubulin occurred as dots on the surfaces of some isolated nuclei in vitro, we detected no microtubule nucleation from isolated nuclei. Clearly, more studies are needed to detect microtubule nucleation from isolated nuclei, but these observations support the contention that microtubule-nucleating capacity is stage specific. RMSs associated with telophase nuclei are important components of the cytokinetic apparatus during meiosis in bryophytes because phragmoplasts develop where opposing RMSs contact one another (Brown and Lemmon, 1988; Shimamura et al., 1998). γ-Tubulin homologs remained on the nuclear surface, although they were no longer located in the remnants of RMS in oryzalin-treated cells (Figures 8E and 8F), suggesting the tight association of γ-tubulin or its complex on the nuclear envelope.

Two Different Localizations of γ-Tubulin: Concentrated at MTOCs and Dispersed along Microtubule Arrays

All studies of γ-tubulin distribution in plant cells have demonstrated the presence of γ-tubulin at suspected microtubule-initiating sites. However, many studies have shown that γ-tubulin is present along organized microtubule arrays as well. γ-Tubulin follows microtubules precisely but is biased toward minus ends (Liu et al., 1993, 1994, 1995; Hoffman et al., 1994; Joshi and Palevitz, 1996). Such findings raise the possibility that plant γ-tubulin is not exclusively a microtubule-initiating site protein and may have additional role(s) in plant cells.

The present study clearly shows that γ-tubulin has two significant different localization patterns: one at MTOC sites (plastid surface, nuclear surface, centrosomes, and POs), and the other along the length of the spindle and phragmoplast arrays of microtubules. In flowering plants that do not have distinct MTOCs, the two different localization patterns might go unnoticed. The anti-microtubule drug study provides additional information about differences in these two localization patterns. Oryzalin treatments induced considerable disorganization of microtubules but had little or no effect on γ-tubulin localization at organelle-based (plastid and nucleus) MTOCs.

γ-Tubulin is present in protein complexes of various sizes in flowering plants (Stoppin-Mellet et al., 2000). The membrane-associated large complex in Arabidopsis has microtubule nucleation activity, but nucleation activity was not observed for the smaller complex that binds laterally to microtubules (Dryková et al., 2003). Two different patterns of γ-tubulin localization in bryophytes also might reflect the existence of multiple post-translational molecular forms and combinations as well as other functions, such as microtubule stabilization, in addition to microtubule nucleation.

In conclusion, data from this study indicate that γ-tubulin is present ubiquitously at sites of microtubule nucleation in land plants and that it is a motile entity that migrates in a cell cycle–specific manner. Furthermore, it is capable of associating with specific organelles and endomembrane systems in the major evolutionary taxa. The plant MTOC can be recognized by the presence of γ-tubulin, and there are transitional stages in extant plants indicating an evolution from corpuscular centriolar centrosomes (as in algal and animal cells) to diffuse association with the nuclear envelope of higher plants. These stages include the concentrated presence of γ-tubulin at acentriolar polar organizers of hepatics and the diffuse association of γ-tubulin with the plastid envelope in monoplastidic mitosis and meiosis of bryophytes. Future efforts need be directed toward identifying the pathway(s) that controls the migration and activity of γ-tubulin in plant cells.

METHODS

Plant Materials

Conocephalum japonicum, *Dumortiera hirsuta* subsp *tatunoi*, and *Makinoa crispata* were collected from natural populations in shady corners of the Higashi-Hiroshima campus of Hiroshima University. *Entodon seductrix* and *Marchantia polymorpha* were collected from long-lived populations growing as weeds in the nursery district of central Louisiana (Forest Hills).

Molecular Cloning

Total DNA of *C. japonicum* was extracted from dried specimens (~200 mg dry weight). Samples were washed several times with distilled water, and excess water was removed from samples with a paper towel. Frozen samples were ground to a powder in liquid nitrogen using a pestle. This powder was suspended in extraction buffer composed of 50 mM Tris-HCl, pH 8.0, 20 mM EDTA, 0.5 M NaCl, 1% (v/v) *N*-lauroylsarcosinate, and 0.2 mg/L proteinase K (TE buffer). Extracted solution was incubated at 37°C for 2 to 3 h. An equal volume of buffered phenol was added to the digestion mixture. The suspension was mixed gently for 10 min and centrifuged for 20 min at 20,000*g*. Then, the upper phase was transferred to a new microtube and mixed gently for 10 min with an equal volume of buffered phenol. The solution was centrifuged for 20 min at 20,000*g*. After transfer of the supernatant to a new tube, an equal volume of chloroform was added, mixed gently, and centrifuged for 5 min at 20,000*g*. After transfer of the upper layer to a new tube, 2.5 volumes of cold absolute ethanol was added, and the solution was mixed gently. The tubes were placed at −20°C for 2 h and centrifuged for 5 min at 20,000*g*. The DNA pellet was rinsed with cold 70% ethanol by inverting the tube several times. After centrifugation for 2 min, the supernatant was discarded and the pellet was dried under vacuum. Then, the DNA was dissolved in 20 to 50 μL of TE buffer. DNA concentration was estimated by ethidium bromide staining after 1% gel electrophoresis. The DNA was stored at −20°C.

Isolated genomic DNA was used as the template for PCR amplification using redundant oligonucleotide primers 294 (5′-GCSGGDCCRTGYGGNAA-3′) and PA4 (5′-NCCNGANCCNGTNCCNCC-3′). DNA was amplified further using primers PS3A (5′-AARGAYGTNTTYTTYTA-3′) and 291 (5′-NCCNGANCCNGTNCCNCC-3′), where N denotes A, C, G or T; S denotes C or G; D denotes A, G, or T; R denotes A or G; and Y denotes C or T. All of these primers were designed to correspond to the conserved amino acid sequences of known γ-tubulins. The resulting amplified DNA was run on an agarose gel, and the specifically amplified band was isolated, purified, and subjected to direct sequencing. Additional primers were designed according to the determined nucleotide sequence. Genomic DNA fragments containing the rest of the γ-tubulin were isolated by vector-annealing PCR amplification. First, the vector pBluescript KS+ (Stratagene, San Diego, CA) was digested with two dif-

ferent restriction enzymes in the multiple cloning sites, yielding a vector with noncohesive ends. The genomic DNA of *C. japonicum* was digested with one of the enzymes used for the digestion of the vector and ligated to the double-digested vector. Then, the resulting vector-conjugated genomic DNA was used as the template for two-step nested PCR amplification.

LA Taq polymerase (Takara Syuzo, Kyoto, Japan) was used for amplification. Primers specific to the γ-tubulin gene sequence that anneal to the genomic DNA were used at one end. General primers located outside of pBluescript KS+ multiple cloning sites were used at the other end for PCR amplification. Genomic DNA fragments containing segments of the γ-tubulin gene were isolated by amplifying the DNA flanked by these primers. Amplified DNA fragments were ligated into the pGEM-T Easy vector using the pGEM-T Easy Vector System (Promega, Madison, WI). Nucleotide sequences of the insert fragments in isolated clones were determined and used to design the primers used to isolate neighboring fragments. At each cloning step, nucleotide sequences of more than one clone were determined and compared visually for PCR errors and the possible presence of more than one γ-tubulin gene. Cloning was repeated using the vector-annealing PCR method until the entire coding sequence was isolated. Specific primers covering the entire coding sequence were designed according to the determined sequence. Four overlapping fragments covering the entire coding region of the γ-tubulin gene were amplified by PCR using genomic DNA as the template. The nucleotide sequence of each fragment was determined on both strands using the PCR direct sequencing method. Nucleotide and amino acid sequences were analyzed using GENETYX-MAC (Software Development, Tokyo, Japan).

For DNA gel blot analysis, genomic DNA of *C. japonicum* was digested with BamHI, HindIII, or PstI, fractionated on a 0.7% agarose gel, and blotted onto a Hybond-N^+ membrane (Amersham Biosciences, Piscataway, NJ). The membrane to which DNA was blotted was hybridized with DNA probe labeled with alkali-labile DIG-11-dUTP (Roche Diagnostics, Mannheim, Germany) according to the manufacturer's instructions with a minor modification: the DIG-11-dUTP was incorporated into probes by means of PCR with KOD-DNA polymerase (Toyobo, Osaka, Japan). A 2.0-kb region of a cloned genomic γ-tubulin gene of *C. japonicum* was amplified by PCR with the primers mossF2 (5′-AACAACTGGGCCAGTGGGTA-3′) and 78 (5′-CTTTTGTGAACCTGTAAC-3′) in the presence of alkali-labile DIG-11-dUTP:unlabeled dTTP at a ratio of 1:10. Hybridization was performed by incubating the membrane and the probe overnight in a 5× SSC (1× SSC is 0.15 M NaCl and 0.015 M sodium citrate) solution containing 50% formamide, 0.1% (w/v) *N*-lauroylsarcosine, 0.02% (w/v) SDS, and 2% (w/v) blocking reagent (Roche Diagnostics) at 42°C. The membrane was washed twice with 2× SSC containing 0.1% SDS solution at room temperature and then twice with 0.1× SSC containing 0.1% SDS solution at 65°C for 15 min each. The labeled probe on the membrane was detected with alkaline phosphatase–labeled anti-digoxigenin antibody (Roche Diagnostics) and with CDP-Star (New England Biolabs, Beverly, MA).

Anti-γ-Tubulin Antibody

A monoclonal anti-γ-tubulin antibody (G9) was used. G9 is one of the monoclonal antibody clones raised against bacterially expressed *Schizosaccharomyces pombe* γ-tubulin (Horio et al., 1999, 2002). The recognized epitopes of these antibodies have been mapped by testing the reactivity of the antibodies to partial fragments of the γ-tubulin. We tested the cross-reactivity of antibodies to the γ-tubulins of other species by protein gel blot analysis. The γ-tubulins used for the test—*Homo sapiens* γ1-tubulin, *Arabidopsis thaliana* γ2-tubulin, the fungus *Aspergillus nidulans*, and the fission yeast *Schizosaccharomyces japonicus*—were expressed in either bacteria or the fission yeast *S. pombe*.

Protein Gel Electrophoresis and Immunoblot Analysis

Sporophytes of *C. japonicum* and *D. hirsuta* were ground with a mortar and pestle in 5 volumes of Laemmli sample buffer (Laemmli, 1970). The extracts were spun in a microcentifuge. The supernatants were boiled and separated on 10% polyacrylamide gels, and proteins were transferred to polyvinylidene difluoride membranes according to Murata-Hori et al. (1998). The membranes were blocked in 1% gelatin at room temperature for 1 h and treated with monoclonal anti-α-tubulin antibody (N356; Amersham) diluted 1:2500 in PBS, monoclonal anti-β-tubulin antibody (N357; Amersham) diluted 1:2500 in PBS, or monoclonal anti-γ-tubulin antibody (G9) diluted 1:500 in PBS. After rinsing in TPBS (0.05% Tween 20 in PBS) secondary antibody, biotinylated anti-mouse IgG (H+L) antibody (BA-2000 Vectastain; Vector Laboratories, Burlingame, CA) was applied in a dilution of 1:200. After rinsing in TPBS, immunoperoxidase staining was performed with an avidin-biotin complex method and 3,3′-diaminobenzidine substrate (Vectastain ABC kit).

Immunofluorescence Microscopy

Sporogenous and spermatogenous tissues were fixed for 60 min with 4.5% formaldehyde in 50 mM PME buffer (50 mM Pipes, 5 mM EGTA, and 1 mM $MgSO_4 \cdot 7H_2O$, pH 6.8) to which 0.1 M sucrose and 1% DMSO had been added. Cell walls were digested for 20 to 30 min with a solution containing 1% β-glucuronidase (Sigma-Aldrich, St. Louis, MO), 1% Pectolyase (Kikkoman, Tokyo, Japan), 0.5% Triton X-100, protease inhibitor cocktail (Boehringer Mannheim, Tokyo, Japan), and 0.3 M mannitol. After a buffer wash, cells were extracted in PME buffer containing 1% Triton X-100 and 1% gelatin for 1 h. After several washes with PME buffer, cells were air-dried on a glass slide and then extracted with methanol at −20°C for 10 min. After washing with PBS for 10 min, cells were incubated with monoclonal anti-γ-tubulin (G9) antibody diluted 1:200 with PBS in a moist chamber for 90 min at 37°C. After a PBS wash, incubation in polyclonal anti-*Vigna* tubulin diluted 1:500 with PBS was performed for 90 min at 37°C. Washed again with PBS, the samples were incubated for 60 min at 37°C with a mixture of Oregon Green 488–labeled goat anti-rabbit IgG (H+L) diluted 1:100 with PBS and Alexa 594 goat anti-mouse IgG (H+L) (Molecular Probes, Eugene, OR) diluted 1:200 with PBS. Slides were mounted using the Slow Fade Antifade kit (Molecular Probes). To stain DNA in nuclei and organelles, 1 μg/L 4′,6-diamidino-2-phenylindole (DAPI) was added in the mounting medium. Preparations were observed using a confocal laser scanning microscope (LSM410; Carl Zeiss, Tokyo, Japan). Images were collected using monochromatic excitation sequentially (Ar, 488 nm; He/Ne, 543 nm; and UV, 365 nm). Although the immunocytochemical images presented here show the triple staining of tubulin, G9, and DAPI, we also examined the double staining of G9 and DAPI to confirm that G9 signals do not derive from the crosstalk of tubulin signals. We present a negative control image in Figure 4I. Similar experiments also were performed in other cases (data not shown).

Preparation of Tubulin and Assembly of Microtubules from Isolated Plastids

Tubulin from bovine brain was isolated with buffer A (20 mM Pipes, 1 mM EGTA, and 0.5 mM $MgSO_4$, pH 6.9) by three cycles of temperature-dependent polymerization and depolymerization (Shelanski et al., 1973). Tubulin then was purified by column chromatography on DEAE-Sephacel. After washing with buffer A containing 0.3 M NaCl, tubulin was eluted with buffer A containing 0.8 M NaCl from this column. The eluate was dialyzed against buffer B (100 mM Pipes, 0.5 mM DTT, 1 mM EGTA, 33% glycerol, 0.1 mM GTP, 0.5 mM $MgSO_4$, and 80 mM NaCl, pH 6.9) at 4°C overnight. GTP was added to 1 mM, and the cycle of temper-

ature-dependent polymerization and depolymerization was repeated twice. The resulting tubulin preparation was stored in liquid nitrogen as a preparation of microtubule-associated protein–free tubulin.

Rhodamine-labeled tubulin was prepared according to Hyman et al. (1991). After polymerization of microtubule-associated protein–free tubulin in buffer B, the preparation was laid on buffer B containing 60% glycerol instead of 33% as a cushion and centrifuged at 154,000*g* for 30 min at 36°C. The precipitated microtubules were suspended to a concentration of 50 mg/mL in a Pipes buffer similar to buffer B except at pH 8.0. Carboxytetramethylrhodamine succinimidyl ester (Molecular Probes) was dissolved in DMSO at 100 mM, and 1/20th volume of microtubule preparation was added under vortexing. After 10 min, the reaction mixture was laid on the cushion buffer with 60% glycerol and centrifuged for 30 min at 154,000*g*. The resulting precipitate of microtubules was depolymerized at 0°C after suspension. The rhodamine-labeled tubulin was purified further by two cycles of temperature-dependent polymerization and depolymerization and then stored in liquid nitrogen.

The lysis medium for sporocytes of *D. hirsuta* consisted of a 0.85 M solution of mannitol, pH 5.5, that contained 0.43% Cellulase Onozuka RS and 0.043% Pectolyase Y23. After incubation at 30°C for 1 h, protoplasts were sedimented by centrifugation for 5 min at 500*g* and washed twice with 0.85 M mannitol. The protoplasts then were ruptured by shearing in chilled medium [10 mM Mes buffer, 0.25 M sucrose, 10 mM NaCl, 2 mM EDTA, 0.15 mM spermine, 0.5 mM spermidine, 20 mM 2-mercaptoethanol, 0.1 mM *p*-4-(2-aminoethyl) benzenesulfonyl fluoride-HCl, and 10 μg/mL leupeptin, pH 6.0] with a glass Teflon homogenizer using 3 to 11 strokes by hand. Plastids released from membrane-lysed protoplasts were precipitated by centrifugation at 1000*g* for 5 min at 4°C. For the detection of activity to organize microtubules, the mixture of rhodamine-labeled tubulin and unlabeled tubulin, at a final concentration of 0.4 mg/mL that never induces spontaneous polymerization, was added to the preparation of isolated plastids. After incubation in polymerization buffer C (50 mM Pipes, 1 mM EGTA, 1 mM $MgSO_4$, 10% DMSO, and 1 mM GTP, pH 6.9) at 27°C for an appropriate time, the reaction mixture was observed by fluorescence microscopy (BX-50; Olympus, Tokyo, Japan) to detect the cluster of microtubule formation. For the observation of γ-tubulin localization in isolated plastids and nuclei, organelles from membrane-lysed protoplasts were fixed for 60 min with 3.6% formaldehyde in 50 mM PME buffer, and immunostaining was performed as described above.

Oryzalin Treatment

Meiotic-stage sporangia of *D. hirsuta* were broken up in 0.3 M sucrose, and the pooled cells were divided between treatments. Oryzalin solution was added to an equal volume of cell suspension to give a final concentration of 20 μM in 0.2% DMSO and 0.3 M sucrose. After 20 min or 2 h, the oryzalin solution was removed and replaced with fixative solution and immunostaining was performed as described above. Oryzalin solutions at concentrations from 1 to 20 μM had similar effects. A control solution using 0.2% DMSO in 0.3 M sucrose showed no difference from 0.3 M sucrose alone (data not shown).

Upon request, materials integral to the findings presented in this publication will be made available in a timely manner to all investigators on similar terms for noncommercial research purposes. To obtain materials, please contact Y. Mineyuki, mineyuk@hiroshima-u.ac.jp.

Accession Numbers

The GenBank accession number for *C. japonicum gtb1* is AF511487. The accession numbers for the sequences shown in Figure 1B are as follows: *Homo sapiens TUG1*, M61764; *Xenopus laevis Xgam*, M63446; *Arabidopsis thaliana TUBG2*, U03990; *Nicotiana tabacum nttug1*, AB051679; *Zea mays GAMTUB*, X78891; *Conocephalum japonicum gtb1*, AF511487; *Physcomitrella patens TubG1*, AF142098; *Anemia phyllitidis tubg*, X69188; *Chlamydomonas reinhardtii* genomic sequence encoding γ-*tubulin*, U31545; *Schizosaccharomyces pombe gtb1+*, X62031; *Aspergillus nidulans mipA*, X15479; and *Saccharomyces cerevisiae TUB4*, U14913.

ACKNOWLEDGMENTS

We thank Masayuki Yamato (University of Tokushima) for preparing G9 antibody and Hiromi Tsubota (Hiroshima University), Natsu Takemura (University of Tokushima), and Miyuki Shimizu (University of Tokushima) for DNA sequences. This work was supported by Grant-in-Aid 200001095 for Japan Society for the Promotion of Science fellows to M.S. and by Grants-in-Aid for Scientific Research B (09044225) and C (12640651) to Y.M. from the Japan Society for the Promotion of Science.

Received August 19, 2003; accepted October 21, 2003.

REFERENCES

Brown, R.C., and Lemmon, B.E. (1982). Ultrastructure of meiosis in the moss *Rhynchostegium serrulatum*. I. Prophasic microtubules and spindle dynamics. Protoplasma **110,** 23–33.

Brown, R.C., and Lemmon, B.E. (1987). Division polarity, development and configuration of microtubule arrays in bryophyte meiosis. I. Meiotic prophase to metaphase I. Protoplasma **137,** 84–99.

Brown, R.C., and Lemmon, B.E. (1988). Cytokinesis occurs at boundaries of domains delimited by nuclear based microtubules in sporocytes of *Conocephalum conicum* (Bryophyta). Cell Motil. Cytoskeleton **11,** 139–146.

Brown, R.C., and Lemmon, B.E. (1990). Polar organizers mark division axis prior to preprophase band formation in mitosis of the hepatic *Reboulia hemisphaerica* (Bryophyta). Protoplasma **156,** 74–81.

Brown, R.C., and Lemmon, B.E. (1992). Polar organizers in monoplastidic mitosis of hepatics (Bryophyta). Cell Motil. Cytoskeleton **22,** 72–77.

Brown, R.C., and Lemmon, B.E. (1993). Diversity of cell division in simple land plants holds clues to evolution of the mitotic and cytokinetic apparatus in higher plants. Mem. Torrey Bot. Club **25,** 45–62.

Brown, R.C., and Lemmon, B.E. (1997). The quadripolar microtubule system in lower land plants. J. Plant Res. **110,** 93–106.

Busby, C.H., and Gunning, B.E.S. (1989). Development of the quadripolar meiotic apparatus in *Funaria* spore mother cells: Analysis by means of anti-microtubule drug treatments. J. Cell Sci. **93,** 267–277.

Dibbayawan, T.P., Harper, J.D.I., and Marc, J. (2001). A γ-tubulin antibody against a plant peptide sequence localizes to cell division specific microtubule arrays and organelles in plants. Micron **32,** 671–678.

Dryková, D., Cenklová, V., Sulimenko, V., Voic, J., Dráber, P., and Binarová, P. (2003). Plant γ-tubulin interacts with αβ-tubulin dimers and forms membrane-associated complexes. Plant Cell **15,** 465–480.

Felix, G.W., Antony, C., Wright, M., and Maro, B. (1994). Centrosome assembly in vitro: Role of γ-tubulin recruitment in *Xenopus* sperm aster formation. J. Cell Biol. **124,** 19–31.

Fuchs, U., Moepps, B., Maucher, H.P., and Schraudolf, H. (1993). Isolation, characterization and sequence of cDNA encoding gamma-tubulin protein from the fern *Anemia phyllitidis* L. Sw. Plant Mol. Biol. **23,** 593–603.

Graham, L.E., and Kaneko, Y. (1991). Subcellular structures of relevance to the origin of land plants (embryophytes) from green algae. Crit. Rev. Plant Sci. **10,** 323–342.

Heidemann, S.R., and McIntosh, J.R. (1980). Visualization of the structure polarity of microtubules. Nature **286,** 517–519.

Hoffman, J.C., Vaughn, K.C., and Joshi, H.C. (1994). Structural and immunocytochemical characterization of microtubule organizing centers in pteridophyte spermatogenous cells. Protoplasma **179,** 46–60.

Horio, T., Basaki, A., Takeoka, A., and Yamato, M. (1999). Lethal level overexpression of γ-tubulin in fission yeast causes mitotic arrest. Cell Motil. Cytoskelton **44,** 284–295.

Horio, T., Kimura, N., Basaki, A., Tanaka, Y., Noguchi, T., Akashi, T., and Tanaka, K. (2002). Molecular and structural characterization of the spindle pole bodies in the fission yeast *Schizosaccharomyces japonicus* var. *japonicus*. Yeast **19,** 1335–1350.

Horio, T., Uzawa, S., Jung, M.K., Oakley, B.R., Tanaka, K., and Yanagida, M. (1991). The fission yeast γ-tubulin is essential for mitosis and is localized at the microtubule organizing centers. J. Cell Sci. **99,** 693–700.

Hyman, A., Drechsel, D., Kellogg, D., Salser, S., Sawin, K.E., Steffen, P., Wordeman, L., and Mitchison, T.J. (1991). Preparation of modified tubulins. Methods Enzymol. **196,** 478–485.

Joshi, H.C., Palacious, M.J., McNamara, L., and Cleveland, D.W. (1992). Gamma-tubulin is a centrosomal protein required for cell cycle-dependent microtubule nucleation. Nature **356,** 80–83.

Joshi, H.C., and Palevitz, B.A. (1996). γ-Tubulin and microtubule organization in plants. Trends Cell Biol. **6,** 41–44.

Joshi, H.C., and Zhou, J. (2001). Gamma tubulin and microtubule nucleation in mammalian cells. Methods Cell Biol. **67,** 179–193.

Khodjakov, A., and Rieder, C.L. (1999). The sudden recruitment of γ-tubulin to the centrosome at the onset of mitosis and its dynamic exchange throughout the cell cycle, do not require microtubules. J. Cell Biol. **146,** 585–596.

Laemmli, U.K. (1970). Cleavage of structural proteins during the assembly of the head of bacteriophage T4. Nature **227,** 680–685.

Lambert, A.M. (1980). The role of chromosomes in anaphase trigger and nuclear envelope activity in spindle formation. Chromosoma **76,** 295–308.

Liu, B., Joshi, H.C., and Palevitz, B.A. (1995). Experimental manipulation of γ-tubulin in *Arabidopsis* using anti-microtubule drugs. Cell Motil. Cytoskelton **31,** 113–129.

Liu, B., Joshi, H.C., Wilson, T.J., Silflow, C.D., Palevitz, B.A., and Snustad, D.P. (1994). γ-Tubulin in Arabidopsis: Gene sequence, immunoblot, and immunofluorescence studies. Plant Cell **6,** 303–314.

Liu, B., Marc, J., Joshi, H.C., and Palevitz, B.A. (1993). A γ-tubulin-related protein associated with the microtubule arrays of higher plants in a cell cycle-dependent manner. J. Cell Sci. **104,** 1217–1228.

Mizuno, K. (1993). Microtubule-nucleation sites on nuclei of higher plant cells. Protoplasma **173,** 77–85.

Motomura, T., Nagasato, C., Komeda, Y., and Okuda, K. (2001). Transient localization of γ-tubulin around the centrioles in the nuclear division of *Boergesenia forbesii* (Siphonocladales, Chlorophyta). J. Phycol. **37,** 783–792.

Murata-Hori, M., Murai, N., Komatsu, S., Uji, Y., and Hosoya, H. (1998). Concentration of singly phosphorylated myosin II regulatory light chain along the cleavage furrow of dividing HeLa cells. Biomed. Res. **19,** 111–115.

Oakley, B.R. (2000). γ-Tubulin. Curr. Top. Dev. Biol. **49,** 27–54.

Oakley, C.E., and Oakley, B.R. (1989). Identification of a γ-tubulin, a new member of the tubulin superfamily encoded by mipA gene of *Aspergillus nidulans*. Nature **338,** 662–664.

Ovenchkina, Y., and Oakley, B.R. (2001). Gamma-tubulin in plant cells. Methods Cell Biol. **67,** 195–212.

Palevitz, B.A. (1993). Morphological plasticity of the mitotic apparatus in plants and its developmental consequences. Plant Cell **5,** 1001–1009.

Pickett-Heaps, J.D. (1975). Green Algae: Structure, Reproduction and Evolution in Selected Genera. (Stamford, CT: Sinauer).

Robbins, R.R. (1984). Origin and behavior of bicentriolar centrosomes in the bryophyte *Riella americana*. Protoplasma **121,** 114–119.

Schnepf, E. (1984). Pre- and postmitotic reorientation of microtubule arrays in young *Sphagnum* leaflets: Transitional stages and initiation sites. Protoplasma **120,** 100–112.

Shaw, S.L., Kamyar, R., and Ehrhardt, D.W. (2003). Sustained microtubule treadmilling in *Arabidopsis* cortical arrays. Science **300,** 1715–1718.

Shelanski, M.L., Gaskin, F., and Cantor, C.R. (1973). Microtubule assembly in the absence of added nucleotides. Proc. Natl. Acad. Sci. USA **70,** 765–768.

Shimamura, M., Deguchi, H., and Mineyuki, Y. (1998). Meiotic cytokinetic apparatus in the formation of the linear spore tetrads of *Conocephalum japonicum* (Bryophyta). Planta **206,** 604–610.

Shimamura, M., Kitamura, A., Mineyuki, Y., and Deguchi, H. (2001). Occurrence of monoplastidic sporocytes and quadripolar microtubule systems in Marchantiales (Bryophyta; Marchantiidae). Hikobia **13,** 551–562.

Shimamura, M., Mineyuki, Y., and Deguchi, H. (2000). Monoplastidic meiosis in *Dumortiera hirsuta* (Bryophyta; Marchantiales). J. Hattori Bot. Lab. **88,** 267–270.

Shimamura, M., Mineyuki, Y., and Deguchi, H. (2003). A review of the occurrence of monoplastidic meiosis in liverworts. J. Hattori Bot. Lab. **94,** 179–186.

Shu, H.B., and Joshi, H.C. (1995). γ-Tubulin can both nucleate microtubule assembly and self-assemble into novel tubular structure in mammalian cells. J. Cell Biol. **130,** 1137–1147.

Silflow, C.D., Liu, B., LaVoie, M., Richardson, E.A., and Palevitz, B.A. (1999). γ-Tubulin in *Chlamydomonas*: Characterization of the gene and localization of the gene product in cells. Cell Motil. Cytoskeleton **42,** 285–297.

Stearns, T., Evans, L., and Kirschner, M.W. (1991). γ-Tubulin is a highly conserved component of the centrosome. Cell **65,** 825–836.

Stearns, T., and Kirschner, M.W. (1994). In vitro reconstruction of centrosome assembly and function: The central role of γ-tubulin. Cell **76,** 623–638.

Stoppin, V., Vantard, M., Schmit, A.C., and Lambert, A.M. (1994). Isolated plant nuclei nucleate microtubule assembly: The nuclear surface in higher plants has centrosome-like activity. Plant Cell **6,** 1099–1106.

Stoppin-Mellet, V., Peter, C., and Lambert, A.M. (2000). Distribution of gamma-tubulin in higher plant cells: Cytosolic gamma-tubulin is part of high molecular weight complexes. Plant Biol. **2,** 290–296.

Vaughn, K.C., and Renzaglia, K.S. (1998). Origin of bicentrioles in Anthocerote spermatogenous cells. In Bryology for the Twenty-First Century, J.W. Bates, N.W. Ashton, and J.D. Duckett, eds (Leeds, UK: Maney Publishing and the British Bryological Society), pp. 189–203.

Zheng, Y., Jung, M.K., and Oakley, B.R. (1991). γ-Tubulin is present in *Drosophila melanogaster* and *Homo sapiens* and is associated with the centrosome. Cell **65,** 817–823.

Zheng, Y., Wong, M.L., Alberts, B., and Mitchison, T. (1995). Nucleation of microtubule assembly by a γ-tubulin-containing ring complex. Nature **378,** 578–583.

γ-Tubulin in Basal Land Plants: Characterization, Localization, and Implication in the Evolution of Acentriolar Microtubule Organizing Centers

Masaki Shimamura, Roy C. Brown, Betty E. Lemmon, Tomohiro Akashi, Koichi Mizuno, Naohisa Nishihara, Ken-Ichi Tomizawa, Katsuhiko Yoshimoto, Hironori Deguchi, Hiroshi Hosoya, Tetsuya Horio and Yoshinobu Mineyuki

Plant Cell 2004;16;45-59; originally published online December 5, 2003;
DOI 10.1105/tpc.016501